Proteomic profile of unstable atheroma plaque: increased neutrophil defensin 1, clusterin and apolipoprotein E levels in carotid secretome

Gemma Aragonès,[1†] Teresa Auguet,[1,2†] Esther Guiu-Jurado,[1] Alba Berlanga,[1] Marta Curriu,[1] Salomé Martinez,[3] Ajla Alibalic,[2] Carmen Aguilar,[1] Esteban Hernández,[4] María-Luisa Camara,[5] Núria Canela,[6] Pol Herrero,[6] Xavier Ruyra,[5] Vicente Martín-Paredero,[4] Cristóbal Richart[1,2*]

[†] These authors contributed equally to this work

[1]Grup de Recerca GEMMAIR - Medicina Aplicada. Departament de Medicina i Cirurgia. Universitat Rovira i Virgili (URV), Institut Investigació Sanitària Pere Virgili (IISPV). Tarragona, Spain.

[2]Servei Medicina Interna, Hospital Universitari Joan XXIII. Tarragona, Spain.

[3]Servei Anatomia Patològica, Hospital Universitari Joan XXIII. Tarragona, Spain.

[4]Servei Angiologia i Cirurgia Vascular, Hospital Universitari Joan XXIII. Tarragona, Spain.

[5]Servei de Cirurgia Cardíaca, Hospital Germans Trias i Pujol. Badalona, Spain.

[6]Group of Research on Omic Methodologies (GROM). Centre for Omic Sciences (COS). Reus, Spain.

***Corresponding author**

Prof. Cristóbal Richart Jurado

Hospital Universitari Joan XXIII (Tarragona). Universitat Rovira i Virgili (URV)

Mallafré Guasch, 4. 43007 Tarragona, Catalonia, Spain

Phone: +34977295833 Fax: +3497722401; email: crichart.hj23.ics@gencat.cat

ABSTRACT

Due to the clinical significance of carotid atherosclerosis, the search for novel biomarkers has become a priority. The aim of the present study was to compare the protein secretion profile of the carotid atherosclerotic plaque (CAP, n=12) and non-atherosclerotic mammary artery (MA, n=10) secretomes. We used a non-targeted proteomic approach which incorporated tandem immunoaffinity depletion, iTRAQ labelling, and nanoflow liquid chromatography coupled to high-resolution mass spectrometry. In total, 162 proteins were quantified, of which 25 showed statistically significant differences in secretome levels between carotid atherosclerotic plaque and non-diseased mammary artery. We found increased levels of neutrophil defensin 1, apolipoprotein E, clusterin and zinc-alpha-2-glycoprotein in CAP secretomes. Results were validated by ELISA assays. Also, differentially secreted proteins are involved in pathways such as focal adhesion and leukocyte transendothelial migration. In conclusion, this study provides a subset of identified proteins that are differently expressed in secretomes of clinical significance.

Keywords: proteomic, atheroma plaque, secretome, atherosclerosis.

INTRODUCTION

Atherosclerosis, the underlying cause of most clinical cardiovascular events, is a chronic and progressive inflammatory disease characterized by the accumulation of lipids and fibrous elements in the large arteries. Its prevalence is assumed to have risen along with the worldwide increase in obesity and diabetes [1,2]. One of the major clinical manifestations of this inflammatory disease is carotid atherosclerosis, which is prevalent and often clinically silent. However, on many occasions, embolisms can cause acute temporary occlusion of the cerebral circulation, resulting in a transient ischemic attack or stroke [3]. With the increasing incidence of atherothrombosis, due to carotid atheroma plaque rupture, the search for novel therapeutic approaches and biomarkers is a priority. Moreover, new biomarkers should have the potential to improve risk-stratification, diagnosis or treatment. Although this pathology has been extensively studied, its molecular mechanisms are not completely understood.

In this regard, the 'omics'-based approaches (such as genomics, transcriptomics, proteomics and metabolomics) have enabled us to make an overall characterization, at the molecular level, of complex global biological systems and their changes in pathological processes. In this context, proteomics has emerged as a useful tool for analysing the proteins involved in the pathogenesis of such diseases as atherosclerosis [4,5]. In the search for potential biomarkers, several proteomic study designs have sought to identify new plasma biomarkers for atherosclerosis and its clinical manifestations [6,7]. The results of these studies are often based on relatively few samples, and so are unable to address the inter-individual variation of candidate biomarkers. Moreover, at the methodological level, direct plasma analysis by proteomic

techniques is limited by challenges such as interference from highly abundant proteins (e.g. albumin and immunoglobulins), which restricts the number of proteins identified/quantified. In this regard, analysis of the secretome has emerged as a new strategy for studying the atheroma plaque in humans [8,9]. The secretome is the sub-set of proteins released by a cell or tissue under certain conditions and shows a narrower dynamic range of proteins than serum or plasma, which means less complexity. Furthermore, studies on tissue secretomes more closely resemble the in vivo situation than cell culture workflows. To date, only a few human arterial secretomes (pathological and non-diseased tissue) have been subject to analysis.

The main objective of this study was to identify potential candidate biomarkers for carotid atherosclerosis. Specifically, we analysed the protein secretion profile of carotid atherosclerotic plaque and non-atherosclerotic mammary secretomes. To evaluate their potential use as atherosclerotic biomarkers, we also studied the functional pathways in which these secreted proteins are involved.

EXPERIMENTAL SECTION

Subjects/Samples

Human carotid atherosclerotic plaques (CAP) were obtained from patients (men, n=12) who underwent carotid endarterectomy at the Angiology and Vascular Surgery Unit of the Hospital Universitari Joan XXIII (Tarragona, Spain). Patients with cerebrovascular ischemia and internal carotid artery stenosis >75% were included, diagnosed by colour Doppler assisted duplex imaging and arteriography. The CAP diagnosis was made by an experienced pathologist following the American Heart Association (AHA) guidelines [10]. Mammary arteries were used as non-atherosclerotic control arteries (MA). Segments of mammary arteries (men, n=10) were obtained during coronary revascularisation surgery at the Cardiovascular Surgery Department of the Germans Trias i Pujol Hospital (Badalona, Spain). Patients who had an acute illness, acute or chronic inflammatory or infective diseases, or malignant neoplastic disease were excluded.

Blood samples were obtained from each individual immediately before surgery and after overnight fasting. Serum was obtained by standard protocols and preserved at -80ºC until use.

The institutional review board approved the study. All participants gave written informed consent for participation in medical research.

Clinical and biochemical assessments

A complete anthropometric, physical examination and biochemical analysis was carried out on each patient. Body height and weight were measured with the patient standing in light clothes and shoeless. Body mass index (BMI) was

calculated as body weight divided by height squared (kg/m^2). Laboratory studies included glucose, insulin, glycated haemoglobin (HbA1c), total cholesterol, high-density lipoprotein cholesterol (HDL-C), low-density lipoprotein cholesterol (LDL-C) and triglycerides, all of which were analysed using a conventional automated analyser. Insulin resistance (IR) was estimated using the homeostasis model assessment of IR (HOMA2-IR) [11].

Tissue processing and secretome preparation

Tissue samples were transported from the surgery to the laboratory in phosphate-buffered saline (PBS) at room temperature. Immediately upon arrival, the tissue was transferred to a Petri dish and washed with PBS. Samples were then cut into similar-sized pieces about 3-5 mm in length and transferred to a 12-well tissue culture plate containing 2ml/well of protein-free Roswell Park Memorial Institute medium (RPMI) (RPMI-1640, Gibco, Invitrogen, N.Y, USA) supplemented with penicillin (100 U/ml), streptomycin (100 µg/ml) and 50 mM HEPES. These procedures were all carried out under a laminar flow hood using sterile equipment. After 24 hours of incubation at 37ºC and 5% of CO_2, the media containing the secreted proteins, the so-called secretome, were collected, aliquoted and stored at -80ºC until analysis. Additionally, a section of each atherosclerotic plaque was placed in formol 10% and further studied by an experienced pathologist from the Hospital Universitari Joan XXIII (Tarragona) following the AHA guidelines [10].

Protein preparation

Secretome samples were concentrated by ultrafiltration using 3kDa Amicon Ultra 0.5mL filters from Millipore in accordance with the manufacturer's instructions. The protein concentration was determined by Bradford's method. A total of 200 µg total protein per sample was run on a self-poured stacking SDS-PAGE gel (12% resolving gel and 4% stacking gel) at 20mA/gel. The electrophoresis was stopped when the front dye had barely passed from the stacking gel (4% acrylamide) into the resolving gel (12% acrylamide), and before the protein mixture had separated into discrete bands in the gel. In this way, all proteins were concentrated in a single band, which removed sample contaminants and made reproducibility for comparison easier. This single concentrated band obtained for every sample was stained using Coomassie Brilliant Blue G-250, excised, cut into small pieces and stored at 4°C in ultrapure water.

Protein digestion

Protein digestion was performed according to Shevchenko et al. with minor variations [12]. Gel pieces were destained using 75% acetonitrile, 25% 0.5M triethylammonium bicarbonate pH 7.9 solution. Then they were de-hydrated by successive washes of 50mM triethylammonium bicarbonate pH 7.9 solution and acetonitrile, and vacuum dried. Subsequently, proteins were reduced using 5mM tris(2-carboxyethyl)phosphine (TCEP) in 50mM triethylammonium bicarbonate pH 7.9 for 1h at 60°C and alkylated with 3.81mM Iodoacetamide (IAA) in the same buffer for 30 min at room temperature in the dark. For digestion, samples were incubated with 15.4 ng/µL sequencing-grade trypsin in 50 mM triethylammonium bicarbonate at pH 7.9 overnight at 37ºC. After

digestion, the peptides were extracted from the gel by elution in a mixture of 50% acetonitrile, 5% formic acid. Tryptic peptides were dried by SpeedVac and re-suspended in 30 ul TEAB 0.5M, pH 7.9.

iTRAQ 8plex labelling and purification

Digested samples were labelled using iTRAQ 8-plex reagents (AB SCIEX). To accommodate all the samples of the study three iTRAQ 8-plex reagent kits are necessary and for this reason samples were equally distributed in three sub-groups (A, B and C) containing both CAP and MA samples to minimize technical variability (Table 1). Hereby, one CAP sample (labelled with 113-tag) was used as normalizer sample for the three iTRAQ groups and to cover all the proteins present in CAP arteries. Quantification results are expressed as ratios of the different labelling tags vs tag 113 and these ratios were used for statistical purposes.

The iTRAQ labelling reaction was performed according to manufacturer's instructions, incubated at room temperature for 120 min and stopped by adding water. After peptides were labelled, they were purified by using a SCX column (Strata® SCX 55 µm, 70 Å, Phenomenex). Then, samples were desalted and concentrated using a C18 Sep-Pak column (Waters, Bedford, MA) previously to nanoLC-MS/MS analysis.

Nano LC chromatography and mass spectrometry

Peptides were separated onto a C-18 reversed phase (RP) nano-column (75 µm I.D.; 15 cm long; 3 µm particle diameter, Nikkyo Technos Co. LTD, Japan)

coupled to a trap nano-column (100 µm I.D.; 2 cm long; 5µm particle diameter, Thermo Fisher Scientific, San Jose, CA, USA).

The three iTRAQ groups (A, B and C) were analysed by triplicate so that a higher number of covered proteins and single peptides could be quantified. For each analysis, 2µg of sample was injected using a continuous acetonitrile gradient consisting of 0–5% B in 4 min, 5-15% B in 60 min, 15-35% B in 60 min and 35-95% B in 10min, which was maintained for 20 min (A = water, 0.1% formic acid; B = acetonitrile, 0.1% formic acid).

In all the analyses a flow rate of 300 nl/min was used to elute peptides for real time ionization and peptide fragmentation on an LTQ-Orbitrap Velos Pro mass spectrometer (Thermo Fisher). An enhanced FT-resolution spectrum (resolution = 30,000 FHMW) followed by MS/MS scan (R=7500 FHMW) from the ten most intense parent ions was analyzed throughout the chromatographic run. The MS/MS scan was acquired in the FT analyzer using an HCD collision cell with normalized collision energy of 45%, a precursor mass window selection of 2 m/z, a charge state rejection of +1 and a dynamic exclusion of 0.5 min.

Protein identification analysis

Tandem mass spectra were extracted and charge state deconvoluted by Proteome Discoverer version 1.4.0.288 (Thermo Fisher Scientific). All MS and MS/MS spectra were analyzed using Mascot search engine node (Matrix Science; version 2.4.1.0). Mascot was set up to search Swissprot 2012_03.fastadatabase (v 2.4, 535248 entries), restricting for human taxonomy (20255 sequences) and assuming trypsin digestion. Two missed cleavages were allowed and an error of 0.80 Da for fragment ion mass and 10.0 ppm for a

parent ion. Oxidation of methionine and acetylation of N-termini were specified as variable modifications, whereas iTRAQ 8-plex and carbamidomethylation of cysteine were set as static modifications. The false discovery rate (FDR) and protein probabilities were calculated by Target Decoy PSM Validator working between 0.01 and 0.05 for strict and relaxed, respectively [9]. For proteins identified with only one peptide, the fragmentation spectra were visually verified. The three technical replicates were analyzed as replicates on Proteome Discover software to obtain a unique report for each iTRAQ group.

Quantitative proteome analysis

Protein quantification was done by calculating the ratios obtained between each iTRAQ mass tag of each unique peptide from a given protein, against tag 113. The quantification is the average value of the ratios obtained for the unique peptides for each protein and was normalized based on protein median. These ratios were exported to an excel spreadsheet for statistical analysis.

ELISA assays

Defrosted secretome samples were centrifuged at 3000 rpm and 4ºC for 15 minutes. Then, they were analysed by enzyme-linked immunosorbent assays (ELISA) following the manufacturer's instructions. Neutrophil defensin 1 (EIAab, Wuhan, China), apopoliprotein E (AssayPro, St. Charles, MO, USA), clusterin (RayBiotech Inc, Norcross, GA, USA) and zinc-alpha-2-glycoprotein (BlueGene Biotech., Shangai, China) were determined in secretome samples.

Statistical analysis

The statistical analysis was performed on Mass Profiler Professional software v.12.1 (Agilent Technologies). For statistical calculations, only these proteins that were quantified in more than 70% samples in almost one condition (CAP and MA) were considered. Differences between groups were calculated using a Student's t test and to avoid false positives, a multiple testing correction using a Benjamini-Hochberg method was used. p values < 0.05 and fold change >1.5 were selected as cut-off values. Principal component analysis (PCA) and hierarchical clustering analysis were performed using Mass Profile Professional software v.12.1 (Agilent Technologies). Pathway analysis was performed using The ConsensusPathDB-human platform. Other statistical calculations were performed using the SPSS software (version 20.0; SPSS, Chicago, IL, USA).

RESULTS

Baseline characteristics of subjects

The clinical characteristics and biochemical measurements of the population studied are shown in Table 2. Patients were classified according to the samples obtained: CAP samples from patients undergoing endarterectomy (n=12) and MA samples from patients undergoing cardiac bypass (n=10). They were all men. The analyses indicated that patients from the CAP and MA groups are of similar ages. Biochemical parameters showed no significant differences between these groups. 80% of MA patients and 83% of CAP patients received lipid-lowering therapy. As expected, hypolipemiant treatment did not show significant differences in both groups (p=0.840).

Protein identification and quantification

In order to assess potential biomarkers for atheromatous plaque progression, we focused on the carotid atherosclerotic secretome and compared it to changes in the mammary secretome. Using a nontargeted proteomic approach, we identified and quantified a total of 162 proteins in the human arterial secretome (Table 3). The analyses of the three ITRAQ groups (A, B and C) were prepared in triplicate so that a higher number of covered proteins and single peptides could be quantified (Figure 1). To study changes in the whole proteome, multivariate statistics (hierarchical clustering analyses and principal component analysis (PCA)) were applied. Figure 2 (A and B) shows that we were able discriminate samples from each group, which suggests that atheromatous plaque progression has a specific secretome. Subsequently, we used univariate statistics to define specific potential biomarkers. We found that

25 proteins exhibit statistically significant differences in secretome levels between carotid atherosclerotic plaque and non-atherosclerotic mammary artery (Table 4). The table shows the role that each protein might play in atherosclerosis according to the literature. Of all the differentially expressed proteins, four had significantly increased levels in CAP secretomes: neutrophil defensin 1, apolipoprotein E, clusterin and zinc-alpha-2-glycoprotein. Multivariate statistics of the 25 proteins that exhibit differences (Figure 2C and 2D) also showed good clusterization and sample discrimination for each group, which suggests that atheromatous plaque progression has a specific secretome.

Validation by ELISA assay

ELISA assays were applied to secretome samples in order to validate the differential release observed by iTRAQ labelling spectrometry. For the verification, we selected proteins with an increase profile in CAP secretomes. We confirmed that neutrophil defensin 1, apolipoprotein E and clusterin levels were significantly increased in CAP secretomes than in mammary artery group (Figure 3A, 3B and 3C). Conversely, the levels of zinc-alpha-2-glycoprotein showed no significant differences between the two secretome groups analysed (Figure 3D).

Pathway analysis

To determine whether differentially expressed proteins belong to specific pathways, we conducted pathway analysis on proteomic data. The ConsensusPathDB-human Platform, which integrates interaction networks in

the Homo sapiens proteome, was used to calculate the pathway impact. Briefly, this platform collates pathways from several public databases of protein interactions, signaling and metabolic pathways, and gene regulation in humans. We applied our analysis to the following databases: KEGG, Reactome, Netpath, Biocarta, HumanCyc and the pathway interaction database (PID), Signalink, Inoh, Wikipathways, Pharmgkb, Humancyc and Ehmn. The use of multiple databases enhances coverage and therefore reduces bias. Only pathways showing two proteins or more in the over-representation analyses and a p value cutoff <0.05 were taken into account (Figure 4). We used this tool for proteins that exhibit statistically significant differences in secretome levels. A list of 10 related pathways was generated. Interestingly, differentially secreted proteins are involved in pathways such as focal adhesion and leukocyte transendothelial migration.

DISCUSSION

Several proteomic approaches have been used to study carotid tissue and understand the mechanisms and progression of atherosclerosis. These studies have identified only a small number of proteins in relatively few samples, and so cannot address the inter-individual variation of candidate biomarkers [13,14]. To date, the human artery secretome has not been extensively analysed so the novelty of this study lies in the fact that we analyzed the proteomic changes that occur in secretomes of carotid atherosclerotic plaque (CAP) and non-atherosclerotic mammary artery (MA). Multivariate statistics revealed overall changes in 162 proteins. Further, when univariate statistics were applied, 25 proteins emerged as potential biomarkers of carotid atherosclerotic plaque. The functional analysis performed in our study corroborated the results of recent studies and revealed that selected proteins were involved in pathways related to vascular disease such as focal adhesion and leukocyte transendothelial migration [15]. Our findings show the potential role of secretome evaluation in carotid atherosclerosis, as a means to determine new possible biomarkers and further study the progression and physiology of the disease.

Of the 25 proteins selected, we will first focus on significantly decreased proteins in carotid atherosclerotic plaque secretomes. We classified the decreased proteins in CAP secretomes into different groups on the basis of their potential role in atherosclerosis, as reported in the literature. Although we found that a significant number of the proteins selected were involved in focal adhesion pathway, these proteins are indirectly related to extracellular matrix and they could be implicated in remodelling of atherosclerotic plaque maturation

such as proteoglycans[16]. The alterations described could indicate tissue remodelling with a loss of elasticity in the artery. Moreover, we observed proteins involved in smooth muscle cell differentiation, contraction, proliferation, migration and focal adhesion pathways, which corroborates that vascular smooth muscle cells play a leading role in plaque progression [17,18]. We also found proteins that were involved in protecting against oxidized stress. One of them, extracellular superoxide dismutase (ecSOD), is an antioxidant enzyme in vascular tissues. It is known that it plays a major role in modulating blood pressure and could prevent endothelial dysfunction [19,20]. Another antioxidant enzyme was peroxiredoxin 2 (Prdx2), which regulates proinflammatory responses, vascular remodelling, and overall oxidative stress [21,22]. A recent study showed that Prdx 2 deficiency in apolipoprotein E–deficient (ApoE/) mice accelerates atherosclerosis by increasing the infiltration of immune cells into plaques [23]. We also observed decreased levels of carbonic anhydrase 1 (CA1) in CAP secretomes. Aamand et al. [24] showed that CA1 plays a role in the generation of vasoactive nitric oxide (NO), which suggests that low levels of CA1 induced impaired NO production and, subsequently, endothelial dysfunction. Finally, in agreement with Martin-Ventura JL et al [25], we also detected a decrease in heat shock protein-70 1A (Hsp70 1A) levels in CAP secretomes. Hsp70 is a chaperone with antiinflammatory and anti-apoptotic properties that improve the viability of stressed vascular smooth muscle cells [26].

The increased proteins in CAP secretomes were neutrophil defensin 1, apolipoprotein E, clusterin and zinc-alpha-2-glycoprotein. As far as neutrophil defensin 1 is concerned, recent studies have revealed that polymorphonuclear

neutrophils participate in the development of atherosclerotic lesions [27–29]. During inflammation, large amounts of intracellular proteins such as neutrophil defensins are released from the activated polymorphonuclear neutrophils [30,31]. These proteins have been found in human atherosclerotic arteries [32,33]. Apart from its role in the inflammation underlying atherosclerosis, this protein inhibits LDL metabolism and fibrinolysis and promotes Lp(a) binding [34]. In addition, some authors [35] have reported that neutrophil defensins could induce leukocyte transendothelial migration and increased foam cell formation. In this regard, according to our results, neutrophil defensin 1 is another key molecule in the pathogenesis of atherosclerosis.

Zinc-alpha-2-glycoprotein (ZAG) is a newly identified adipokine and it has not been studied on atheroma plaque yet. In agreement with our findings, several studies have shown that serum ZAG levels are upregulated in a variety of pathological processes involving endothelial dysfunction [36–38]. However, immunoassay data did not show similar profiles as the ones obtained in spectrometry experiments. This protein has been quantified by mass spectrometry using only a 1 unique peptide. In this sense, it has been described in the literature that this sequence could be easily modified [39,40] and these changes could affect the quantification by mass spectrometry or ELISA detection. Otherwise, the quantitative changes detected by mass spectrometry referred to a very minor difference.

As far as the role of clusterin in atherosclerotic lesions is concerned, other authors studying the atheroma plaque have reported similar results to ours [41,42]. Indeed, clusterin is upregulated in a wide variety of clinical situations including aging, diabetes and atherosclerosis [43,44]. Although the role of clusterin in

atherosclerosis remains unknown, several studies have shown that clusterin distribution in human aorta is increased as this disease progress [42,45].

Human apolipoprotein E (apoE) plays an important role in the metabolism of lipids, including cholesterol, and promotes the clearance of atherogenic lipoproteins such as very low density lipoprotein (VLDL) and chylomicron remnants from the circulation [46]. In addition, the expression of apoE in macrophages plays an important anti-atherogenic role by promoting cholesterol efflux from cells in the arterial wall [47]. Recent studies have indicated that the regulation of apoE expression from macrophages is under the control of several signaling pathways. ApoE secretion was stimulated by several molecules such as apolipoprotein A-I, HDL, ATP binding cassette transporter (ABCA1), protein kinase A, intracellular calcium and microtubular network [48]. In addition, the function of apoE is linked with both proinflammatory and antiinflammatory cytokines [49]. Therefore, under pathological conditions, the expression of apoE could be upregulated by macrophages in the arterial wall. In our study, one explanation for high levels of apoE in carotid atherosclerotic secretomes finding could be that this molecule may act as a protective factor.

We should point out the following drawbacks of our study. First, we used mammary arteries as controls since previous studies have shown a lower incidence of atherosclerosis. Although non-diseased carotid arteries would be the best choice, unfortunately they were not available. Second, our results were obtained in homogeneous groups of men. Therefore, they cannot be extrapolated to other population groups with mixed genders or associated metabolic diseases. Third, our patients were in treatment. Although we cannot

exclude the influence of drugs on our results, this study design provided information of real clinical situation during necessary lipid lowering therapy. Finally, another limitation of the study was the sample size due to the fact the difficulty in obtaining human artery samples. Despite that, our high sensitive method evidences a very wide spectrum of proteins in CAP and MA secretomes which was verified by ELISA assays. Further studies would be useful to validate our findings.

CONCLUSIONS

In conclusion, our results indicate the potential role of secretome analysis in carotid atherosclerosis, as a means to identify new possible biomarkers and further study the progression and physiology of the disease. By means of iTRAQ labelling spectrometry, some proteins involved in focal adhesion, oxidative stress, inflammation and endothelial dysfunction, among others, were differentially identified. Prospective studies are needed to confirm what profile of secreted proteins could be useful targets for diagnosing and treating carotid atherosclerosis.

Acknowledgments

This study was supported by the Ministerio de Ciencia e Innovación of the government of Spain (grant number SAF 2008-02278, to C.R.), the Fondo de Investigación Sanitaria (grant number PI13/00468, to T.A.), the Agència de Gestió d'Ajuts Universitaris i de Recerca (AGAUR 2009 SGR 959 to C.R.), the Grup de Recerca en Medicina Aplicada URV (2010PFR-URV-B2-14 to C.R.) and the Fundación Biociencia.

Conflict of interest

The authors have no conflict of interests to declare.

Abbreviations: BMI, body mass index; CVD, cardiovascular disease; HbA1c, glycosylated hemoglobin; HDL-C, high density lipoprotein; HOMA2-IR, homeostasis model assessment of insulin resistance; CAP, carotid atherosclerotic plaque; MA, mammary artery; LDL-C, low density lipoprotein; PBS, phosphate buffered saline; RPMI, protein-free Roswell Park Memorial Institute medium.

REFERENCES

(1) Hansson, G. K. Inflammation, atherosclerosis, and coronary artery disease. *N. Engl. J. Med.* **2005**, *352* (16), 1685–1695.

(2) Lusis, A. J. Atherosclerosis. *Nature* **2000**, *407* (6801), 233–241.

(3) Stöllberger, C.; Chnupa, P.; Abzieher, C.; Länger, T.; Finsterer, J.; Klem, I.; Hartl, E.; Wehinger, C.; Schneider, B. Mortality and rate of stroke or embolism in atrial fibrillation during long-term follow-up in the embolism in left atrial thrombi (ELAT) study. *Clin. Cardiol.* **2004**, *27* (1), 40–46.

(4) Ramsey, S. A.; Gold, E. S.; Aderem, A. A systems biology approach to understanding atherosclerosis. *EMBO Mol. Med.* **2010**, *2* (3), 79–89.

(5) Döring, Y.; Noels, H.; Weber, C. The use of high-throughput technologies to investigate vascular inflammation and atherosclerosis. *Arterioscler. Thromb. Vasc. Biol.* **2012**, *32* (2), 182–195.

(6) Gerszten, R. E.; Asnani, A.; Carr, S. A. Status and prospects for discovery and verification of new biomarkers of cardiovascular disease by proteomics. *Circ. Res.* **2011**, *109* (4), 463–474.

(7) Vasan, R. S. Biomarkers of cardiovascular disease: molecular basis and practical considerations. *Circulation* **2006**, *113* (19), 2335–2362.

(8) De la Cuesta, F.; Barderas, M. G.; Calvo, E.; Zubiri, I.; Maroto, A. S.; Darde, V. M.; Martin-Rojas, T.; Gil-Dones, F.; Posada-Ayala, M.; Tejerina, T.; et al. Secretome analysis of atherosclerotic and non-atherosclerotic arteries reveals dynamic extracellular remodeling during pathogenesis. *J. Proteomics* **2012**, *75* (10), 2960–2971.

(9) Alvarez-Llamas, G.; Martín-Rojas, T.; de la Cuesta, F.; Calvo, E.; Gil-Dones, F.; Dardé, V. M.; Lopez-Almodovar, L. F.; Padial, L. R.; Lopez, J.-A.; Vivanco, F.; et al. Modification of the secretion pattern of proteases, inflammatory mediators, and extracellular matrix proteins by human aortic valve is key in severe aortic stenosis. *Mol. Cell. Proteomics* **2013**, *12* (9), 2426–2439.

(10) Stary, H. C. Natural history and histological classification of atherosclerotic lesions: an update. *Arterioscler. Thromb. Vasc. Biol.* **2000**, *20* (5), 1177–1178.

(11) Terra, X.; Auguet, T.; Broch, M.; Sabench, F.; Hernández, M.; Pastor, R. M.; Quesada, I. M.; Luna, A.; Aguilar, C.; del Castillo, D.; et al. Retinol binding protein-4 circulating levels were higher in nonalcoholic fatty liver disease vs. histologically normal liver from morbidly obese women. *Obesity (Silver Spring).* **2013**, *21* (1), 170–177.

(12) Shevchenko, A.; Wilm, M.; Vorm, O.; Mann, M. Mass spectrometric sequencing of proteins silver-stained polyacrylamide gels. *Anal. Chem.* **1996**, *68* (5), 850–858.

(13) Lepedda, A. J.; Cigliano, A.; Cherchi, G. M.; Spirito, R.; Maggioni, M.; Carta, F.; Turrini, F.; Edelstein, C.; Scanu, A. M.; Formato, M. A proteomic approach to differentiate histologically classified stable and unstable plaques from human carotid arteries. *Atherosclerosis* **2009**, *203* (1), 112–118.

(14) Olson, F. J.; Sihlbom, C.; Davidsson, P.; Hulthe, J.; Fagerberg, B.; Bergström, G. Consistent differences in protein distribution along the longitudinal axis in symptomatic carotid atherosclerotic plaques. *Biochem. Biophys. Res. Commun.* **2010**, *401* (4), 574–580.

(15) Rocchiccioli, S.; Pelosi, G.; Rosini, S.; Marconi, M.; Viglione, F.; Citti, L.; Ferrari, M.; Trivella, M. G.; Cecchettini, A. Secreted proteins from carotid endarterectomy: an untargeted approach to disclose molecular clues of plaque progression. *J. Transl. Med.* **2013**, *11*, 260.

(16) Talusan, P.; Bedri, S.; Yang, S.; Kattapuram, T.; Silva, N.; Roughley, P. J.; Stone, J. R. Analysis of intimal proteoglycans in atherosclerosis-prone and atherosclerosis-resistant human arteries by mass spectrometry. *Mol. Cell. Proteomics* **2005**, *4* (9), 1350–1357.

(17) Yang, C.; Canton, G.; Yuan, C.; Ferguson, M.; Hatsukami, T. S.; Tang, D. Advanced human carotid plaque progression correlates positively with flow shear stress using follow-up scan data: an in vivo MRI multi-patient 3D FSI study. *J. Biomech.* **2010**, *43* (13), 2530–2538.

(18) Cicha, I.; Wörner, A.; Urschel, K.; Beronov, K.; Goppelt-Struebe, M.; Verhoeven, E.; Daniel, W. G.; Garlichs, C. D. Carotid plaque vulnerability: a positive feedback between hemodynamic and biochemical mechanisms. *Stroke.* **2011**, *42* (12), 3502–3510.

(19) Gongora, M. C.; Qin, Z.; Laude, K.; Kim, H. W.; McCann, L.; Folz, J. R.; Dikalov, S.; Fukai, T.; Harrison, D. G. Role of extracellular superoxide dismutase in hypertension. *Hypertension* **2006**, *48* (3), 473–481.

(20) Fukai, T.; Siegfried, M. R.; Ushio-Fukai, M.; Griendling, K. K.; Harrison, D. G. Modulation of extracellular superoxide dismutase expression by angiotensin II and hypertension. *Circ. Res.* **1999**, *85* (1), 23–28.

(21) Yang, C.-S.; Lee, D.-S.; Song, C.-H.; An, S.-J.; Li, S.; Kim, J.-M.; Kim, C. S.; Yoo, D. G.; Jeon, B. H.; Yang, H.-Y.; et al. Roles of peroxiredoxin II in the regulation of proinflammatory responses to LPS and protection against endotoxin-induced lethal shock. *J. Exp. Med.* **2007**, *204* (3), 583–594.

(22) Choi, M. H.; Lee, I. K.; Kim, G. W.; Kim, B. U.; Han, Y.-H.; Yu, D.-Y.; Park, H. S.; Kim, K. Y.; Lee, J. S.; Choi, C.; et al. Regulation of PDGF signalling and vascular remodelling by peroxiredoxin II. *Nature* **2005**, *435* (7040), 347–353.

(23) Park, J.-G.; Yoo, J.-Y.; Jeong, S.-J.; Choi, J.-H.; Lee, M.-R.; Lee, M.-N.; Hwa Lee, J.; Kim, H. C.; Jo, H.; Yu, D.-Y.; et al. Peroxiredoxin 2 deficiency exacerbates atherosclerosis in apolipoprotein E-deficient mice. *Circ. Res.* **2011**, *109* (7), 739–749.

(24) Aamand, R.; Dalsgaard, T.; Jensen, F. B.; Simonsen, U.; Roepstorff, A.; Fago, A. Generation of nitric oxide from nitrite by carbonic anhydrase: a possible link between metabolic activity and vasodilation. *Am. J. Physiol. Heart Circ. Physiol.* **2009**, *297* (6), H2068–H2074.

(25) Martin-Ventura, J. L.; Leclercq, A.; Blanco-Colio, L. M.; Egido, J.; Rossignol, P.; Meilhac, O.; Michel, J.-B. Low plasma levels of HSP70 in patients with carotid atherosclerosis are associated with increased levels of proteolytic markers of neutrophil activation. *Atherosclerosis* **2007**, *194* (2), 334–341.

(26) Johnson, A. D.; Berberian, P. A.; Tytell, M.; Bond, M. G. Differential distribution of 70-kD heat shock protein in atherosclerosis. Its potential role in arterial SMC survival. *Arterioscler. Thromb. Vasc. Biol.* **1995**, *15* (1), 27–36.

(27) Naruko, T.; Ueda, M.; Haze, K.; van der Wal, A. C.; van der Loos, C. M.; Itoh, A.; Komatsu, R.; Ikura, Y.; Ogami, M.; Shimada, Y.; et al. Neutrophil infiltration of culprit lesions in acute coronary syndromes. *Circulation* **2002**, *106* (23), 2894–2900.

(28) Avanzas, P.; Arroyo-Espliguero, R.; Cosín-Sales, J.; Aldama, G.; Pizzi, C.; Quiles, J.; Kaski, J. C. Markers of inflammation and multiple complex stenoses (pancoronary plaque vulnerability) in patients with non-ST segment elevation acute coronary syndromes. *Heart* **2004**, *90* (8), 847–852.

(29) Ovbiagele, B.; Lynn, M. J.; Saver, J. L.; Chimowitz, M. I. Leukocyte count and vascular risk in symptomatic intracranial atherosclerosis. *Cerebrovasc. Dis.* **2007**, *24* (2-3), 283–288.

(30) Rehaume, L. M.; Hancock, R. E. W. Neutrophil-derived defensins as modulators of innate immune function. *Crit. Rev. Immunol.* **2008**, *28* (3), 185–200.

(31) Rodríguez-García, M.; Oliva, H.; Climent, N.; García, F.; Gatell, J. M.; Gallart, T. Human immature monocyte-derived dendritic cells produce and secrete alpha-defensins 1-3. *J. Leukoc. Biol.* **2007**, *82* (5), 1143–1146.

(32) Barnathan, E. S.; Raghunath, P. N.; Tomaszewski, J. E.; Ganz, T.; Cines, D. B.; Higazi A al-R. Immunohistochemical localization of defensin in human coronary vessels. *Am. J. Pathol.* **1997**, *150* (3), 1009–1020.

(33) Nassar, H.; Lavi, E.; Akkawi, S.; Bdeir, K.; Heyman, S. N.; Raghunath, P. N.; Tomaszewski, J.; Higazi, A. A.-R. alpha-Defensin: link between inflammation and atherosclerosis. *Atherosclerosis* **2007**, *194* (2), 452–457.

(34) Higazi, A. A.; Lavi, E.; Bdeir, K.; Ulrich, A. M.; Jamieson, D. G.; Rader, D. J.; Usher, D. C.; Kane, W.; Ganz, T.; Cines, D. B. Defensin stimulates the binding of lipoprotein (a) to human vascular endothelial and smooth muscle cells. *Blood* **1997**, *89* (12), 4290–4298.

(35) Quinn, K. L.; Henriques, M.; Tabuchi, A.; Han, B.; Yang, H.; Cheng, W.-E.; Tole, S.; Yu, H.; Luo, A.; Charbonney, E.; et al. Human neutrophil peptides mediate endothelial-monocyte interaction, foam cell formation, and platelet activation. *Arterioscler. Thromb. Vasc. Biol.* **2011**, *31* (9), 2070–2079.

(36) Leal, V. O.; Lobo, J. C.; Stockler-Pinto, M. B.; Farage, N. E.; Abdalla, D. S. P.; Leite, M.; Mafra, D. Is zinc-α2-glycoprotein a cardiovascular protective factor for patients undergoing hemodialysis? *Clin. Chim. Acta.* **2012**, *413* (5-6), 616–619.

(37) Tedeschi, S.; Pilotti, E.; Parenti, E.; Vicini, V.; Coghi, P.; Montanari, A.; Regolisti, G.; Fiaccadori, E.; Cabassi, A. Serum adipokine zinc α2-glycoprotein and lipolysis in cachectic and noncachectic heart failure patients: relationship with neurohormonal and inflammatory biomarkers. *Metabolism.* **2012**, *61* (1), 37–42.

(38) Stepan, H.; Philipp, A.; Roth, I.; Kralisch, S.; Jank, A.; Schaarschmidt, W.; Lössner, U.; Kratzsch, J.; Blüher, M.; Stumvoll, M.; et al. Serum levels of the adipokine zinc-α2-glycoprotein are increased in preeclampsia. *J. Endocrinol. Invest.* **2012**, *35* (6), 562–565.

(39) Araki, T.; Gejyo, F.; Takagaki, K.; Haupt, H.; Schwick, H. G.; Bürgi, W.; Marti, T.; Schaller, J.; Rickli, E.; Brossmer, R. Complete amino acid sequence of human plasma Zn-alpha 2-glycoprotein and its homology to histocompatibility antigens. *Proc. Natl. Acad. Sci. U. S. A.* **1988**, *85* (3), 679–683.

(40) Wagner, S. A.; Beli, P.; Weinert, B. T.; Schölz, C.; Kelstrup, C. D.; Young, C.; Nielsen, M. L.; Olsen, J. V; Brakebusch, C.; Choudhary, C. Proteomic analyses reveal divergent ubiquitylation site patterns in murine tissues. *Mol. Cell. Proteomics* **2012**, *11* (12), 1578–1585.

(41) Mackness, B.; Hunt, R.; Durrington, P. N.; Mackness, M. I. Increased immunolocalization of paraoxonase, clusterin, and apolipoprotein A-I in

the human artery wall with the progression of atherosclerosis. *Arterioscler. Thromb. Vasc. Biol.* **1997**, *17* (7), 1233–1238.

(42) Ishikawa, Y.; Akasaka, Y.; Ishii, T.; Komiyama, K.; Masuda, S.; Asuwa, N.; Choi-Miura, N. H.; Tomita, M. Distribution and synthesis of apolipoprotein J in the atherosclerotic aorta. *Arterioscler. Thromb. Vasc. Biol.* **1998**, *18* (4), 665–672.

(43) Trougakos, I. P.; Poulakou, M.; Stathatos, M.; Chalikia, A.; Melidonis, A.; Gonos, E. S. Serum levels of the senescence biomarker clusterin/apolipoprotein J increase significantly in diabetes type II and during development of coronary heart disease or at myocardial infarction. *Exp. Gerontol. 37* (10-11), 1175–1187.

(44) Antonelou, M. H.; Kriebardis, A. G.; Stamoulis, K. E.; Trougakos, I. P.; Papassideri, I. S. Apolipoprotein J/Clusterin is a novel structural component of human erythrocytes and a biomarker of cellular stress and senescence. *PLoS One* **2011**, *6* (10), e26032.

(45) Baiersdörfer, M.; Schwarz, M.; Seehafer, K.; Lehmann, C.; Heit, A.; Wagner, H.; Kirschning, C. J.; Koch-Brandt, C. Toll-like receptor 3 mediates expression of clusterin/apolipoprotein J in vascular smooth muscle cells stimulated with RNA released from necrotic cells. *Exp. Cell Res.* **2010**, *316* (20), 3489–3500.

(46) Karagiannides, I.; Abdou, R.; Tzortzopoulou, A.; Voshol, P. J.; Kypreos, K. E. Apolipoprotein E predisposes to obesity and related metabolic dysfunctions in mice. *FEBS J.* **2008**, *275* (19), 4796–4809.

(47) Bellosta, S.; Mahley, R. W.; Sanan, D. A.; Murata, J.; Newland, D. L.; Taylor, J. M.; Pitas, R. E. Macrophage-specific expression of human apolipoprotein E reduces atherosclerosis in hypercholesterolemic apolipoprotein E-null mice. *J. Clin. Invest.* **1995**, *96* (5), 2170–2179.

(48) Kockx, M.; Jessup, W.; Kritharides, L. Regulation of Endogenous Apolipoprotein E Secretion by Macrophages. *Arterioscler. Thromb. Vasc. Biol.* **2008**, *28* (6), 1060–1067.

(49) Zhang, H.; Wu, L.-M.; Wu, J. Cross-Talk between Apolipoprotein E and Cytokines. *Mediators Inflamm.* **2011**, *2011*, 1–10.

FIGURE LEGENDS

Figure 1. Analysis of the three ITRAQ groups (A, B and C) prepared in triplicate so that a higher number of covered proteins and unique peptides were quantified.

Figure 2. Proteomic analysis in CAP and MA secretome samples. Heat map representation of hierarchical clustering of molecular features found in each sample of two groups (**A** represents quantified proteins and **C** statistically significant proteins). The scale from -2.4 blue (low abundance) to +2.4 red (high abundance) represents this normalized abundance in arbitrary units. The CAP group is represented as red samples and MA secretomes as blue samples. Tridimensional principal component analysis (PCA) was used before (**B**) and after (**D**) Student's unpaired t-test. The CAP group is represented as red spots and the MA group as blue spots. CAP, carotid atherosclerotic plaque; MA, mammary artery secretome.

Figure 3. Protein validation by ELISA assays. Neutrophil defensin 1 (**A**), apolipoprotein E (**B**), clusterin (**C**) and zinc-alpha-2-glycoprotein (**D**) levels in secretome samples.

Figure 4. The ConsensusPathDB-human platform integrating interaction networks in Homo sapiens proteome was used to calculate pathway impact. Pathway analysis was conducted on proteins that exhibit statistically significant differences in secretome levels. Minimum overlap with input protein = 2 and p-value cutoff < 0.05.

Table 1. Sample labelling and distribution in three iTRAQ groups (A, B and C).

iTRAQ groups	Labelling	Sample Type
A	113	CAP*
	114	MA
	115	CAP
	116	MA
	117	CAP
	118	CAP
	119	MA
	121	CAP
B	113	CAP*
	114	MA
	115	MA
	116	CAP
	117	MA
	118	MA
	119	CAP
	121	MA
C	113	CAP*
	114	CAP
	115	CAP
	116	CAP
	117	CAP
	118	MA
	119	MA
	121	MA

CAP, carotid atherosclerotic plaque; MA, control mammary artery. *This sample was added in all groups in order to normalize the quantification results that are expressed as ratios of the different labelling tags vs tag 113.

Table 2. Clinical baseline characteristics of the cohort studied

	CAP group (n=12) Mean ± SD	**MA group** (n=10) Mean ± SD
Age (years)	68,83 ± 6,39	67,00 ± 9,99
BMI (kg/m^2)	28,06 ± 3,26	30,64 ± 1,27
Glucose (mg/dl)	129,17 ± 49,75	118,88 ± 45,64
HbA1c (%)	6,39 ± 1,07	7,03 ± 1,38
Insulin (mUI/L)	8,29 ± 4,95	10,47 ± 6,89
HOMA2-IR	1,01 ± 0,67	1,59 ± 0,97
Triglycerides (mg/dL)	112,00 ± 44,67	113,50 ± 27,97
Cholesterol (mg/dl)	122,10 ± 36,22	130,07 ± 24,96
HDL-C (mg/dL)	29,08 ± 7,20	24,33 ± 4,76
LDL-C (mg/dL)	70,73 ± 27,49	78,56 ± 19,48

CAP, carotid atherosclerotic plaque; MA, control mammary artery; BMI, body mass index; HbA1c, glycosylated haemoglobin; HOMA2-IR, homeostatic model assessment 2-insulin resistance; HDL-C, high density lipoprotein; LDL-C, low density lipoprotein. Data are expressed as mean ± SD. $p<0.05$ are considered statistically significant. HOMA-2 is calculated using the HOMA Calculator version 2.2.2 (http://www.dtu.ox.ac.uk).

Table 3. Protein identified in human carotid plaque secretome

Swiss-Prot ID	Protein Name	Coverage %	Unique Peptides*	Peptides	PSMs	MW [kDa]	calc. pI
P01834	Ig kappa chain C region	80.19	5	5	119	11.6	5.87
P68871	Hemoglobin subunit beta	65.99	5	8	440	16.0	7.28
P0CG05	Ig lambda-2 chain C regions	62.26	3	5	55	11.3	7.24
Q01995	Transgelin	55.72	11	11	64	22.6	8.84
P0CG04	Ig lambda-1 chain C regions	46.23	1	3	43	11.3	7.87
P02042	Hemoglobin subunit delta	44.22	3	6	222	16.0	8.05
P02768	Serum albumin	42.53	28	28	793	69.3	6.28
P08670	Vimentin	42.49	16	19	183	53.6	5.12
P69905	Hemoglobin subunit alpha	35.21	5	5	146	15.2	8.68
P02647	Apolipoprotein A-I	33.71	9	9	49	30.8	5.76
P0CG48	Polyubiquitin-C	32.85	2	2	8	77.0	7.66
P02675	Fibrinogen beta chain	31.98	12	12	175	55.9	8.27
P60709	Actin. cytoplasmic 1	28.80	1	9	103	41.7	5.48
P63261	Actin. cytoplasmic 2	28.80	1	9	101	41.8	5.48
P02649	Apolipoprotein E	28.39	8	8	30	36.1	5.73
P32119	Peroxiredoxin-2	27.78	4	5	27	21.9	5.97
P01860	Ig gamma-3 chain C region	27.59	2	8	162	41.3	7.9
Q96KK5	Histone H2A type 1-H	27.34	3	3	11	13.9	10.89
P01598	Ig kappa chain V-I region EU	26.85	2	2	6	11.8	8.44
P02679	Fibrinogen gamma chain	26.71	11	11	75	51.5	5.62
P00738	Haptoglobin	26.35	10	10	40	45.2	6.58
P01765	Ig heavy chain V-III region TIL	26.09	2	2	6	12.3	9.13
P02787	Serotransferrin	25.50	16	16	125	77.0	7.12
P01766	Ig heavy chain V-III region BRO	25.00	2	2	30	13.2	6.57
P01620	Ig kappa chain V-III region SIE	24.77	2	2	14	11.8	8.48
P01857	Ig gamma-1 chain C region	23.94	2	7	157	36.1	8.19
P02743	Serum amyloid P-component	23.77	5	5	18	25.4	6.54
P01625	Ig kappa chain V-IV region Len	21.93	2	2	2	12.6	7.93
P09493	Tropomyosin alpha-1 chain	21.48	3	8	25	32.7	4.74
P60174	Triosephosphate isomerase	21.33	5	5	9	30.8	5.92
P01871	Ig mu chain C region	19.91	8	8	37	49.3	6.77
P07951	Tropomyosin beta chain	19.72	2	7	27	32.8	4.7
P63267	Actin. gamma-enteric smooth muscle	19.41	1	7	78	41.8	5.48
P00338	L-lactate dehydrogenase A chain	19.28	4	6	28	36.7	8.27
P59665	Neutrophil defensin 1	19.15	2	2	10	10.2	6.99
P18206	Vinculin	19.14	18	18	51	123.7	5.66
P01859	Ig gamma-2 chain C region	19.02	2	6	142	35.9	7.59
P01700	Ig lambda chain V-I region HA	18.75	2	2	11	11.9	8.91
P00915	Carbonic anhydrase 1	18.01	5	5	54	28.9	7.12
P01876	Ig alpha-1 chain C region	17.85	2	5	61	37.6	6.51
P01717	Ig lambda chain V-IV region Hil	17.76	1	1	1	11.5	6.51
P01617	Ig kappa chain V-II region TEW	17.70	1	2	6	12.3	6

P62805	Histone H4	17.48	2	2	2	11.4	11.36
P05452	Tetranectin	17.33	3	3	3	22.5	5.67
P01593	Ig kappa chain V-I region AG	16.67	1	1	6	12.0	5.99
P02792	Ferritin light chain	16.57	3	3	13	20.0	5.78
P21333	Filamin-A	15.72	30	30	139	280.6	6.06
P06310	Ig kappa chain V-II region	15.04	1	2	6	14.7	9.25
P01877	Ig alpha-2 chain C region	15.00	1	4	50	36.5	6.1
P06733	Alpha-enolase	14.75	6	6	33	47.1	7.39
P02671	Fibrinogen alpha chain	14.67	12	12	119	94.9	6.01
Q06830	Peroxiredoxin-1	14.57	2	3	14	22.1	8.13
P01023	Alpha-2-macroglobulin	14.18	18	18	101	163.2	6.46
O43707	Alpha-actinin-4	13.83	5	10	33	104.8	5.44
P01009	Alpha-1-antitrypsin	13.64	6	6	66	46.7	5.59
P01024	Complement C3	13.47	19	19	78	187.0	6.4
P02545	Prelamin-A/C	13.25	8	8	30	74.1	7.02
P01011	Alpha-1-antichymotrypsin	13.24	5	5	41	47.6	5.52
P06396	Gelsolin	12.15	9	9	44	85.6	6.28
P08294	Extracellular superoxide dismutase [Cu-Zn]	12.08	2	2	3	25.8	6.61
P62942	Peptidyl-prolyl cis-trans isomerase FKBP1A	12.04	1	1	1	11.9	8.16
P02760	Protein AMBP	11.93	3	3	10	39.0	6.25
P12814	Alpha-actinin-1	11.88	3	8	25	103	5.41
P51884	Lumican	11.83	4	4	24	38.4	6.61
P05109	Protein S100-A8	11.83	1	1	3	10.8	7.03
P37802	Transgelin-2	11.56	2	2	5	22.4	8.25
P07737	Profilin-1	11.43	1	1	4	15.0	8.27
P30086	Phosphatidylethanolamine-binding protein 1	10.70	1	1	3	21.0	7.53
P07195	L-lactate dehydrogenase B chain	10.48	1	3	5	36.6	6.05
P04075	Fructose-bisphosphate aldolase A	10.44	4	4	19	39.4	8.09
P10909	Clusterin	9.80	3	3	16	52.5	6.27
P02144	Myoglobin	9.74	1	1	6	17.2	7.68
P01008	Antithrombin-III	9.70	4	4	9	52.6	6.71
P02652	Apolipoprotein A-II	9.00	1	1	1	11.2	6.62
P07339	Cathepsin D	8.98	3	3	5	44.5	6.54
P06703	Protein S100-A6	8.89	1	1	11	10.2	5.48
P02766	Transthyretin	8.84	1	1	3	15.9	5.76
P04406	Glyceraldehyde-3-phosphate dehydroge-nase]	8.66	2	2	11	36.0	8.46
P60660	Myosin light polypeptide 6	8.61	1	1	3	16.9	4.65
P31949	Protein S100-A11	8.57	1	1	10	11.7	7.12
P02763	Alpha-1-acid glycoprotein 1	8.46	2	2	2	23.5	5.02
P35542	Serum amyloid A-4 protein	8.46	1	1	2	14.7	9.07
P01605	Ig kappa chain V-I region Lay	8.33	1	1	5	11.8	7.96
P00325	Alcohol dehydrogenase 1B	8.27	3	3	6	39.8	8.29
P04433	Ig kappa chain V-III region VG (Fragment)	7.83	1	1	7	12.6	4.96
P04083	Annexin A1	7.8	2	2	2	38.7	7.02
P36955	Pigment epithelium-derived factor	7.66	3	3	6	46.3	6.38

P17661	Desmin	7.66	1	4	21	53.5	5.27
P52565	Rho GDP-dissociation inhibitor 1	7.35	1	1	1	23.2	5.11
P14618	Pyruvate kinase isozymes M1/M2	7.34	3	3	11	57.9	7.84
P06888	Ig lambda chain V-I region EPS	7.34	1	1	11	11.4	9.29
P23528	Cofilin-1	7.23	1	1	1	18.5	8.09
O60814	Histone H2B type 1-K	7.14	1	1	2	13.9	10.32
P07355	Annexin A2	7.08	2	2	4	38.6	7.75
P0C0L4	Complement C4-A	7.00	10	10	19	192.7	7.08
P00558	Phosphoglycerate kinase 1	6.71	2	2	7	44.6	8.1
P13797	Plastin-3	6.67	3	4	9	70.8	5.6
P12883	Myosin-7	6.67	11	11	18	223	5.8
P00441	Superoxide dismutase [Cu-Zn]	6.49	1	1	6	15.9	6.13
P02790	Hemopexin	6.28	3	3	13	51.6	7.02
P06702	Protein S100-A9	6.14	1	1	2	13.2	6.13
P61626	Lysozyme C	6.08	1	1	7	16.5	9.16
P23284	Peptidyl-prolyl cis-trans isomerase B	6.02	1	1	1	23.7	9.41
P08758	Annexin A5	5.94	2	2	9	35.9	5.05
P78417	Glutathione S-transferase omega-1	5.81	1	1	1	27.5	6.6
P08107	Heat shock 70 kDa protein 1A/1B	5.77	3	3	12	70.0	5.66
P63104	14-3-3 protein zeta/delta	5.71	1	1	2	27.7	4.79
P06732	Creatine kinase M-type	5.51	1	1	3	43.1	7.25
P02794	Ferritin heavy chain	4.92	1	1	2	21.2	5.55
P08571	Monocyte differentiation antigen CD14	4.8	1	1	1	40.1	6.23
P00450	Ceruloplasmin	4.79	4	4	12	122.1	5.72
Q6NZI2	Polymerase I and transcript release factor	4.62	1	1	1	43.4	5.6
P04004	Vitronectin	4.6	2	2	2	54.3	5.8
P05155	Plasma protease C1 inhibitor	4.6	2	2	3	55.1	6.55
P02751	Fibronectin	4.44	7	7	28	262.5	5.71
P29401	Transketolase	4.33	2	2	2	67.8	7.66
P62258	14-3-3 protein epsilon	4.31	1	1	2	29.2	4.74
P04264	Keratin. type II cytoskeletal 1	4.04	3	3	6	66.0	8.12
P25311	Zinc-alpha-2-glycoprotein	4.03	1	1	3	34.2	6.05
P68366	Tubulin alpha-4A chain	4.02	1	1	3	49.9	5.06
P00918	Carbonic anhydrase 2	3.85	1	1	1	29.2	7.4
P08603	Complement factor H	3.82	4	4	8	139.0	6.61
P02774	Vitamin D-binding protein	3.8	1	1	1	52.9	5.54
Q01518	Adenylyl cyclase-associated protein 1	3.79	1	1	2	51.9	8.06
Q13642	Four and a half LIM domains protein 1	3.72	1	1	2	36.2	8.97
P08238	Heat shock protein HSP 90-beta	3.59	2	2	8	83.2	5.03
P26038	Moesin	3.47	2	2	2	67.8	6.4
P07451	Carbonic anhydrase 3	3.46	1	1	1	29.5	7.34
P19827	Inter-alpha-trypsin inhibitor heavy chain H1	3.4	2	2	5	101.3	6.79
Q14624	Inter-alpha-trypsin inhibitor heavy chain H4	3.33	3	3	5	103.3	6.98
P13796	Plastin-2	3.03	1	2	9	70.2	5.43
P51911	Calponin-1	3.03	1	1	3	33.1	9.07
P40925	Malate dehydrogenase. cytoplasmic	2.99	1	1	2	36.4	7.36

P40121	Macrophage-capping protein	2.87	1	1	4	38.5	6.19
A6NIK2	Leucine-rich repeat-containing protein 10B	2.74	1	1	1	32.7	7.36
P20774	Mimecan	2.68	1	1	1	33.9	5.63
P02749	Beta-2-glycoprotein 1	2.61	1	1	5	38.3	7.97
P55058	Phospholipid transfer protein	2.43	1	1	1	54.7	7.01
P37837	Transaldolase	2.37	1	1	1	37.5	6.81
P18428	Lipopolysaccharide-binding protein	2.29	1	1	1	53.3	6.7
P06727	Apolipoprotein A-IV	2.27	1	1	2	45.4	5.38
P04217	Alpha-1B-glycoprotein	2.22	1	1	1	54.2	5.86
P00488	Coagulation factor XIII A chain	2.19	1	1	1	83.2	6.09
P16930	Fumarylacetoacetase	1.91	1	1	1	46.3	6.95
P02765	Alpha-2-HS-glycoprotein	1.91	1	1	2	39.3	5.72
P01042	Kininogen-1	1.86	1	1	3	71.9	6.81
P04003	C4b-binding protein alpha chain	1.84	1	1	1	67.0	7.3
Q12805	EGF-containing fibulin-like extracellular matrix protein 1	1.83	1	1	1	54.6	5.07
P00751	Complement factor B	1.83	1	1	4	85.5	7.06
P07602	Proactivator polypeptide	1.72	1	1	2	58.1	5.17
P04040	Catalase	1.71	1	1	1	59.7	7.39
P02748	Complement component C9	1.61	1	1	5	63.1	5.59
Q05682	Caldesmon	1.51	1	1	1	93.2	5.66
O75083	WD repeat-containing protein 1	1.32	1	1	2	66.2	6.65
P00747	Plasminogen	1.23	1	1	1	90.5	7.24
Q8N436	Inactive carboxypeptidase-like protein X2	1.19	1	1	2	85.8	6.87
P00734	Prothrombin	1.13	1	1	2	70.0	5.9
Q9Y490	Talin-1	0.94	2	2	3	269.6	6.07
P35579	Myosin-9	0.82	1	1	1	226.4	5.6
P04114	Apolipoprotein B-100	0.77	3	3	8	515.3	7.05
P01031	Complement C5	0.6	1	1	3	188.2	6.52
P07996	Thrombospondin-1	0.6	1	1	1	129.3	4.94

The proteins included in this table met all identification criteria laid out in the Methods section. Proteins are arranged according to the % coverage of target protein by identified peptides. *Unique peptide: the number of identified unique peptides subjected to quantification for the given protein. PSM, peptide spectrum match; MW, molecular weight; calc. pI, predicted isoelectric point.

Table 4. Secretome proteins differ significantly between CAP and MA group

Swiss-Prot ID	Protein	Gene name	*Role in atherosclerosis	Ratio	P-value	Effect
P51911	Calponin-1	CNN1	SMC differentiation	0.30	0.0024	decreased
P09493	Tropomyosin-1 alpha	TPM1	SMC differentiation	0.35	<0.001	decreased
P00325	Alcohol dehydrogenase 1B	ADH1B	-	0.41	<0.001	decreased
Q01995	Transgelin	TAGLN	SMC differentiation	0.21	<0.001	decreased
P07951	Tropomyosin beta chain	TMP2	SMC differentiation	0.31	<0.001	decreased
P21333	Filamin-A	FLNA	Focal adhesion	0.31	<0.001	decreased
P30086	Phosphatidylethanolamine-binding protein 1	PEBP1	-	0.50	0.0013	decreased
P63267	Actin, gamma-enteric smooth muscle	ACTG2	Focal adhesion	0.40	0.0036	decreased
P18206	Vinculin	VCL	Focal adhesion	0.33	<0.001	decreased
P08670	Vimentin	VIM	Focal adhesion	0.58	0.0027	decreased
O43707	Alpha-actinin-4	ACTN4	Focal adhesion	0.30	<0.001	decreased
P12814	Alpha-actinin-1	ACTN1	Focal adhesion	0.42	<0.001	decreased
P08107	Heat shock protein-70 1A	HSPA1A	Inflammation	0.48	<0.001	decreased
P04075	Fructose-bisphosphate aldolase A	ALDOA	-	0.59	0.0018	decreased
P00915	Carbonic anhydrase 1	CA1	Endothelial dysfunction	0.49	0.0013	decreased
P32119	Peroxiredoxin-2	PRDX2	Antioxidant enzyme	0.51	0.0014	decreased
P40925	Malate dehydrogenase	MDH1	-	0.56	0.0091	decreased
P04264	Keratin, type II cytoskeletal 1	KRT1	-	0.47	0.0091	decreased
P08294	Extracellular superoxide dismutase	SOD3	Antioxidant enzyme	0.58	<0.001	decreased
Q9Y490	Talin-1	TLN1	Focal adhesion	0.63	0.0099	decreased
P59665	Neutrophil defensin 1	DEFA1	Leukocyte migration	1.91	0.0366	increased
P01766	Ig heavy chain V-III region BRO	-	-	1.71	<0.001	increased
P02649	Apolipoprotein E	APOE	Lipid transport	1.61	0.0018	increased
P10909	Clusterin	CLU	Lipid transport	2.28	<0.001	increased
P25311	Zinc-alpha-2-glycoprotein	AZGP1	Endothelial dysfunction	1.66	0.0099	increased

Student's unpaired t-test was used. To avoid false positives, a multiple testing correction using a Benjamini-Hochberg method was also used. P-value<0.05 and fold change>1.5 were selected as cut-off values. *Role in atherosclerosis refers to data reported in the literature.

Graphical abstract

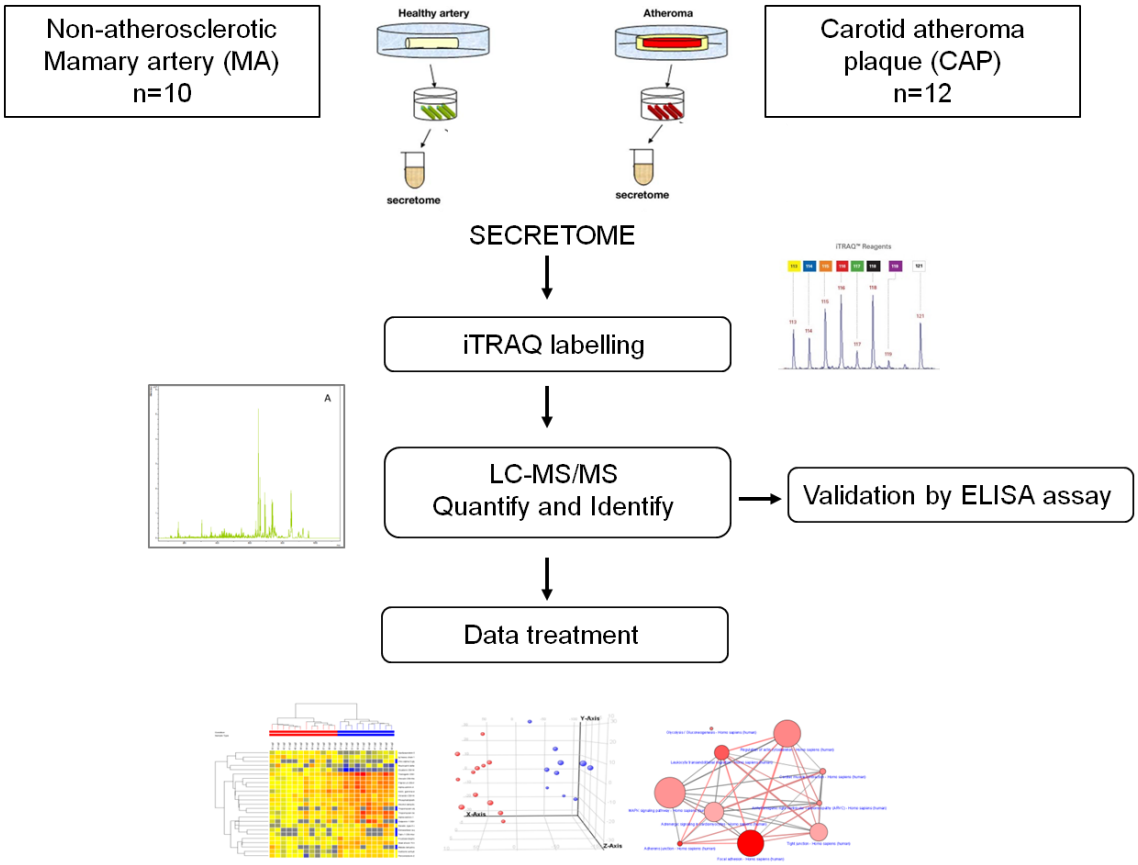

Figure 1.

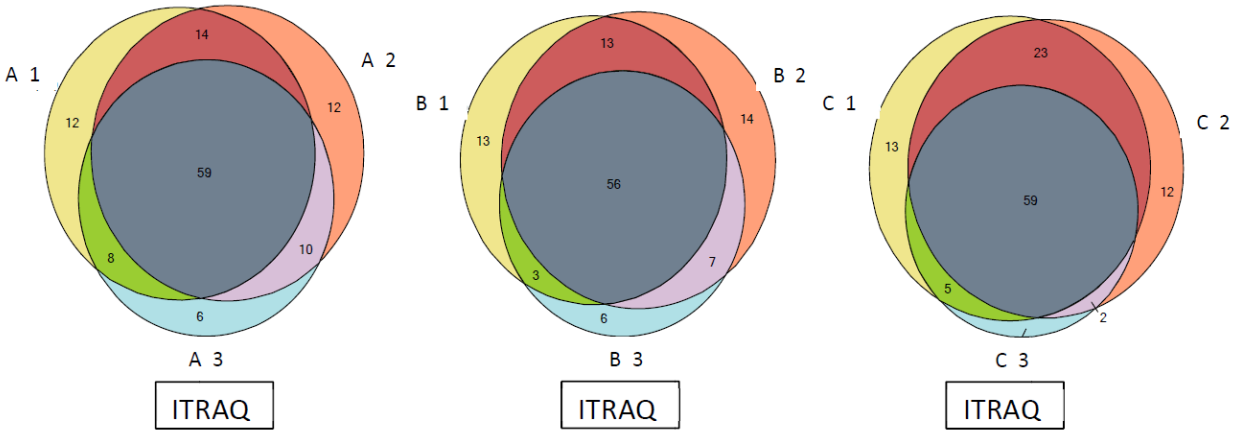
A 1
A 2
A 3
14
12
12
59
8
10
6
ITRAQ
B 1
B 2
B 3
13
13
14
56
3
7
6
ITRAQ
C 1
C 2
C 3
23
13
12
59
5
2
ITRAQ

Figure 2.

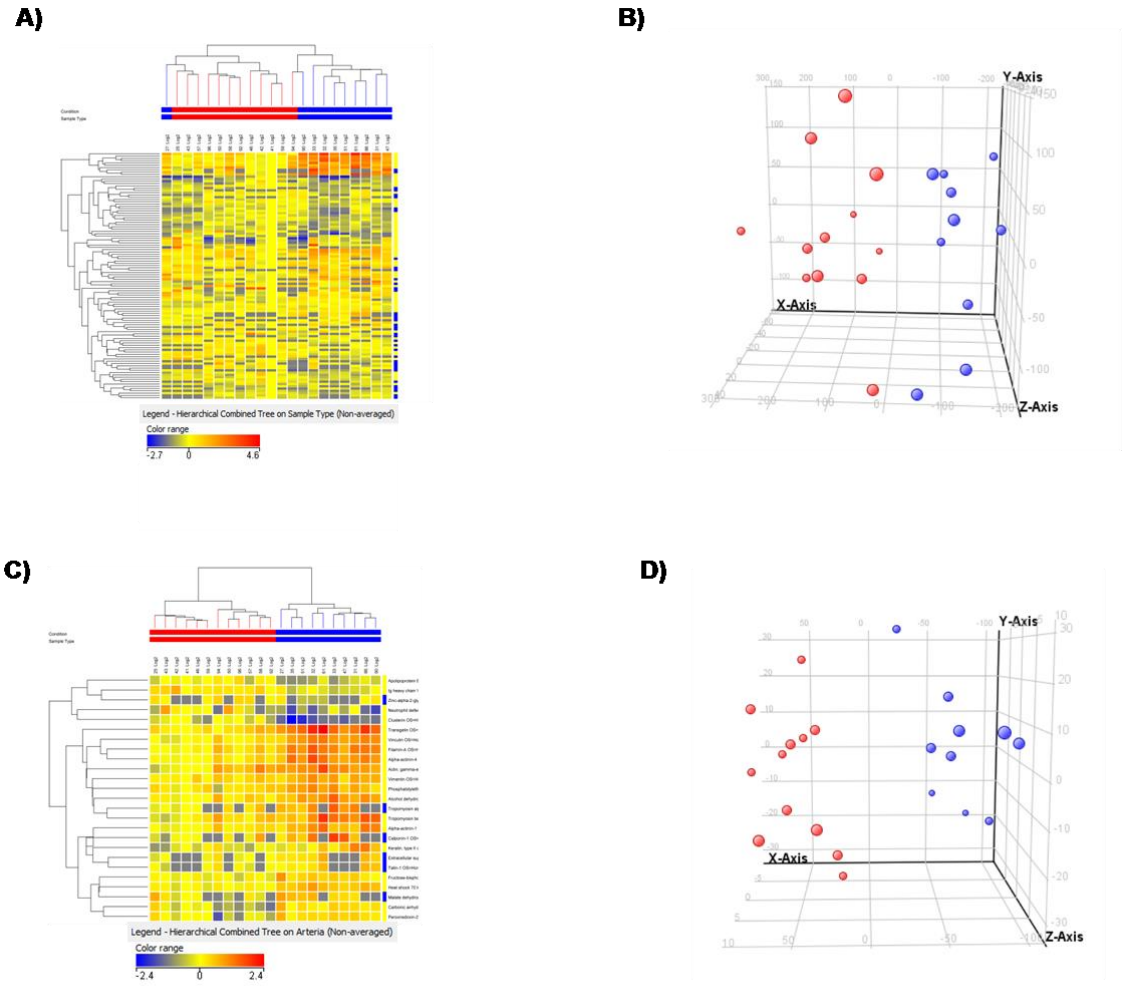
A)
Legend - Hierarchical Combined Tree on Sample Type (Non-averaged)
Color range
-2.7
0
4.6
B)
Y-Axis
X-Axis
Z-Axis
C)
Legend - Hierarchical Combined Tree on Arteria (Non-averaged)
Color range
-2.4
0
2.4
D)
Y-Axis
X-Axis
Z-Axis

Figure 3.

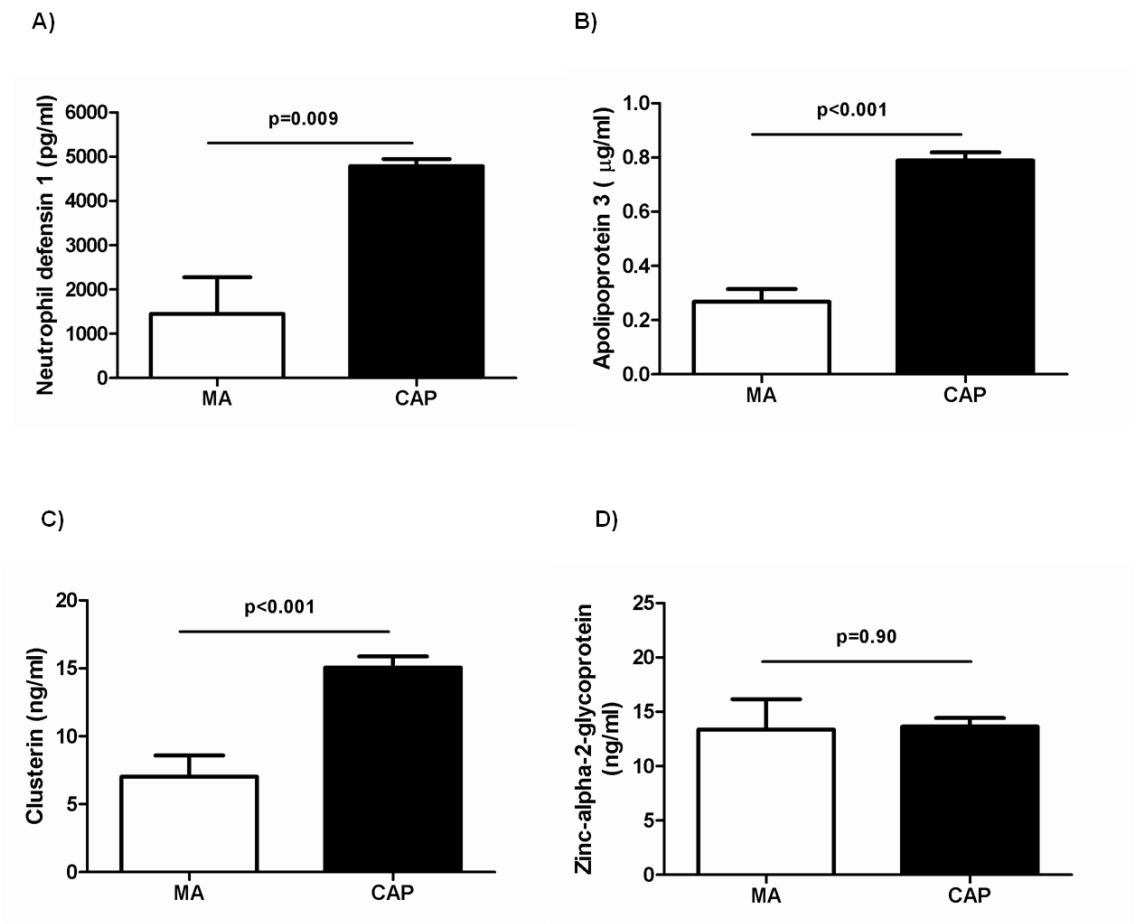
A)
Neutrophil defensin 1 (pg/ml)
6000
5000
4000
3000
2000
1000
0
p=0.009
MA
CAP
B)
Apolipoprotein 3 (μg/ml)
1.0
0.8
0.6
0.4
0.2
0.0
p<0.001
MA
CAP
C)
Clusterin (ng/ml)
20
15
10
5
0
p<0.001
MA
CAP
D)
Zinc-alpha-2-glycoprotein (ng/ml)
25
20
15
10
5
0
p=0.90
MA
CAP

Figure 4.

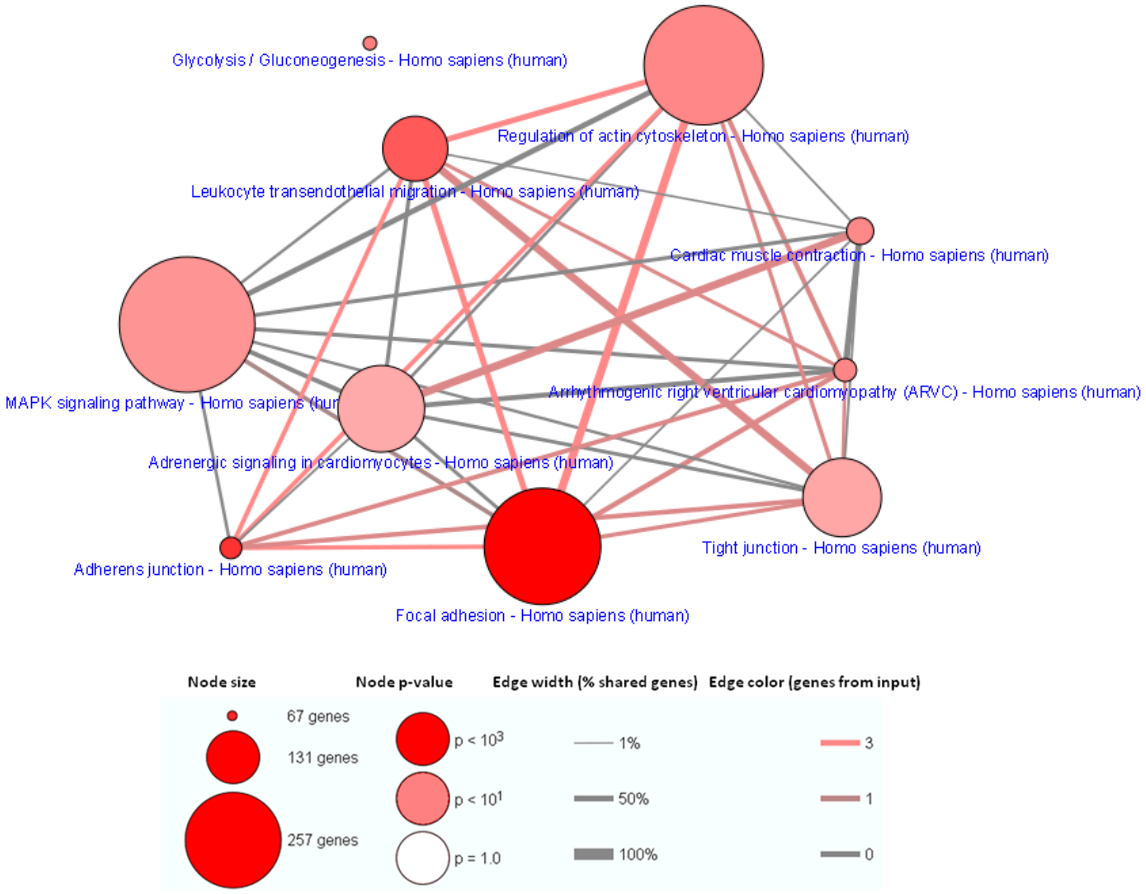
Glycolysis / Gluconeogenesis - Homo sapiens (human)
Regulation of actin cytoskeleton - Homo sapiens (human)
Leukocyte transendothelial migration - Homo sapiens (human)
Cardiac muscle contraction - Homo sapiens (human)
MAPK signaling pathway - Homo sapiens (hum
Arrhythmogenic right ventricular cardiomyopathy (ARVC) - Homo sapiens (human)
Adrenergic signaling in cardiomyocytes - Homo sapiens (human)
Tight junction - Homo sapiens (human)
Adherens junction - Homo sapiens (human)
Focal adhesion - Homo sapiens (human)
Node size
67 genes
131 genes
257 genes
Node p-value
p < 10^3
p < 10^1
p = 1.0
Edge width (% shared genes)
1%
50%
100%
Edge color (genes from input)
3
1
0